Electronic Supplementary Material (ESI) for Journal of Materials Chemistry A.

Electronic Supplementary Information (ESI)

A microporous hydrogen-bonded organic framework with amine sites for selective recognition of small molecules

Hailong Wang, Hui Wu, Jinglan Kan, Ganggang Chang, Zizhu Yao, Bin Li, Wei Zhou,*
Shengchang Xiang, John Cong-Gui Zhao and Banglin Chen*

Experimental section

General remarks

All reagents and solvents were used directly as received from the chemical supplier without further purification. The precursors, 1,3,5-tribromo-2,4,6-trimethylbenzene and 1,3,5-tricyano-2,4,6-trimethylbenzene, were prepared according to the reported procedures with slight modifications (Scheme S1).[1,2] The organic ligand (TDTTB) was synthesized based on the reported procedure.[3]

Scheme S1. Schematic synthesis of the building block (TDTTB) for the self-assembly of HOF-9.

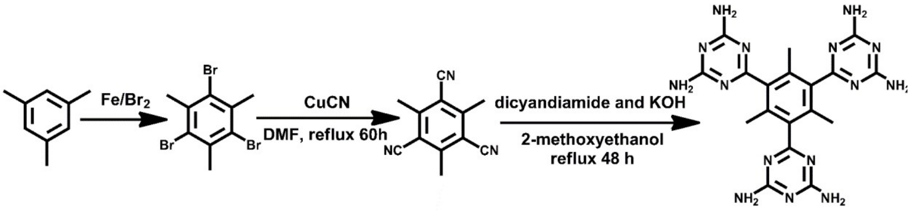

Synthesis of HOF-9

Synthesis of 1,3,5-tribromo-2,4,6-trimethylbenzene. To a 100 mL flask containing iron powder (1.0 g, 17.9 mmol) and bromine (50.0 g, 312.5 mmol) bathed in the ice-water, mesitylene (6.7 g, 55.7 mmol) was slowly added over 2 hours. The resulting reaction mixture was stirred for additional 72 hours and then suspended in 200 mL ice water. After the pH value of the suspension being adjusted to about 3.0 using NaOH (4M) solution, the precipitate was filtered and washed by water and ethanol. The yield of 1,3,5-tribromo-2,4,6-trimethylbenzene was 16.9 g (85%). The product was used directly without further purification. ^{1}H NMR ($CDCl_3$, 500 MHz) δ(ppm): 2.65 (s, 9H).

Synthesis of 1,3,5-tricyano-2,4,6-trimethylbenzene. 1,3,5-Tribromo-2,4,6-trimethylbenzene (4.0 g, 11.2 mmol), CuCN (5.0 g, 55.9 mmol), and dimethyl formamide (50 mL) were placed in a 150 mL Schlenk flask. The mixture was refluxed for 60 hours under nitrogen atmosphere, and then suspended into 300 mL water. Ethylenediamine (10 mL) was added, and the resulting mixture was stirred at 100°C for 1 h and filtered. The precipitate was extracted with dichloromethane (3 × 150 mL). The combined organic phase was dried with $MgSO_4$, filtered, and evaporated in vacuum. The residue was repeatedly purified by chromatography on silica using a hexane/CH_2Cl_2

(1:1) as eluent, giving 1,3,5-tricyano-2,4,6-trimethylbenzene 0.9 g with a yield of 41%. ^{1}H NMR ($CDCl_3$, 500 MHz) δ(ppm): 2.81 (s, 9H).

Synthesis of 1,3,5-tris(2,4-diamino-1,3,5-triazin-6-yl)-2,4,6-trimethylbenzene (TDTTB), HOF-9 and HOF-9⊐Py. A mixture of 1,3,5-tricyano-2,4,6-trimethylbenzene (0.6 g, 3.1 mmol), dicyandiamide (3.0 g, 35.7 mmol), and KOH (0.4 g, 7.1 mmol) in methyl cellosolve (40 mL) was stirred and refluxed for 48 h under nitrogen atmosphere. After the resulting mixture was cooled to room temperature, the precipitate was filtered and washed with water and ethanol, respectively, then dried under vacuum at 90°C to give a white solid (1.1 g) with a yield of 80%. ^{1}H NMR (DMSO-d_6, 500 MHz) δ(ppm): 6.69 (s, 12H), 1.86 (s, 9H). ^{13}C NMR (DMSO-d_6, 500.0 MHz) δ (ppm): 174.81, 167.19, 137.22, 129.43, and 16.78. Colourless block-shaped crystals of HOF-9 were grown from 5 mL DMSO/H_2O (v:v = 9:1) solution containing TDTTB (0.080 g). By gradually adding the Py into the mother liquid of HOF-9 for ten days, the HOF-9⊐Py single crystals were obtained after one and a half months.

Selective adsorption of HOF-9 towards liquid aromatics

The high performance liquid chromatography (HPLC) grade organic solvents were used without further purification. HOF-9 (20 mg) was added to a glass vial containing 2 mL organic solvent, including Py, benzene, toluene, *o*-xylene, *m*-xylene, *p*-xylene, Py/toluene (v:v = 1:1), Py/bezene (v:v = 1:1), and Py/*p*-xylene (v:v = 1:1) mixture. After soaking for 72 hours, the treated HOF-9 was filtered and washed three times using dry pentane. The treated HOF-9 was dissolved in DMSO-d_6 and investigated using ^{1}H NMR spectroscopy.

Physical measurements

NMR spectra were recorded on a Varian INOVA 500 MHz spectrometer at room temperature. The internal standard of $\delta = 7.26$ ppm was employed in ^{1}H NMR spectra collected in $CDCl_3$ solution. Internal standards of $\delta = 2.50$ ppm and $\delta = 39.5$ ppm were used in ^{1}H NMR and ^{13}C NMR spectra, respectively, recorded in DMSO-d_6 solution. Thermogravimetric analysis (TGA) was performed on a Shimadzu TGA-50 thermogravimetric analyzer under N_2 atmosphere with a heating rate of 3°C/min.

Powder X-ray diffraction (PXRD) data were collected on a Rigaku Ultima IV diffractometer.

Before the gas sorption measurements, as-synthesized crystals of HOF-9 were exchanged with dry acetone six times and then evacuated to 6 μmmHg at room temperature to generate activated HOF-9a. Gas sorption isotherms of activated HOF-9a were measured on a Micromeritics ASAP 2020 surface area analyzer, and the measurement temperature was maintained at 196 K with a dry ice-acetone slurry, 273 K with an ice-water bath, and 296 K with a water bath in an air-conditioned 23 ^{o}C laboratory.

Crystallographic investigation

Crystallographic data of HOF-9⊃Py single crystal was collected on an Oxford Diffraction SuperNova diffractometer with Cu Kα radiation (λ = 1.54184 Å) at 100.00(16) K. The structure was solved using the direct method (SHELXS-97) and refined utilizing full-matrix least-squares (SHELXL-97) on F^2.[4] In addition, we note that the ‘SQUEEZE’ command was employed because of the seriously disordered solvent molecules in the HOF-9⊃Py pores. In order to compare with the structure of HOF-9⊃Py, the crystallographic data of as-synthesized HOF-9[3] single crystal was also collected at 100.00(16) K by using the same single crystal diffractometer in this work. Powder X-ray diffraction (PXRD) data were collected on a Rigaku Ultima IV diffractometer. The PXRD pattern of activated HOF-9a sample can be indexed using a hexagonal system, and the space group was identified as *P*-62*c*. The structure was then solved using the direct method. Finally, Rietveld refinement was performed on the powder XRD pattern using the GSAS package.[5] Refinement on the lattice parameters, background, and peak profile, as well as the atomic positions of C and N with constraints applied on C-C and C-N bond lengths yielded the agreement factors of $R_{\mathrm{wp}} = 0.1105$ and $R_{\mathrm{p}} = 0.0771$, which strongly supports the validity of the structure solution. The positions of H atoms were estimated from the geometry and the common length of C-H bonds of the benzene ring and N-H bonds of the primary amine. Selected crystallographic data and pertinent information for these three phases are summarized in Table S2. CCDC 1529718, 1438257 and 1438256 for HOF-9, HOF-9⊃Py and HOF-9a, respectively, contain the supplementary crystallographic data for this paper. These data can be obtained free of charge from the Cambridge Crystallographic Data Centre *via* www.ccdc.cam.ac.uk/data_request/cif.

Calculation details

Density-functional theory calculations. First-principles density-functional theory (DFT) calculations were performed using the Quantum-Espresso package.[6] A semi-empirical addition of dispersive forces to conventional DFT[7] was included in the calculation to account for van der Waals interactions. We used Vanderbilt-type ultrasoft pseudopotentials and the generalized gradient approximation (GGA) with the Perdew-Burke-Ernzerhof (PBE) exchange correlation. A cutoff energy of 544 eV and a 2×2×2 k-point mesh (generated using the Monkhosrt-Pack scheme) were found to be enough for total energy to converge within 0.01 meV/atom. We first optimized the HOF-9 and HOF-9a structures. The DFT-D optimized structures agree fairly well with the experimentally determined crystal structures. Py, benzene, and CO_2 molecule were then introduced to the corresponding optimized HOF structure, followed by a full structural relaxation. To obtain the Py or benzene binding energy, a single Py or benzene molecule placed in a supercell with the same cell dimensions was also relaxed as a reference. The static binding energy (at $T = 0$ K) was calculated using: $E_B = E(\text{HOF-9}) + E(\text{Py or benzene}) - E(\text{HOF-9}\supset\text{Py or HOF-9}\supset\text{benzene})$. To obtain the gas binding energy, a CO_2 gas molecule placed in a HOF-9a supercell with the same cell dimensions was also relaxed as a reference. The static binding energy was then calculated using $E_B = E(\text{HOF-9a}) + E(CO_2) - E(\text{HOF-9a}\supset CO_2)$.

IAST calculation. Adsorption isotherms and gas selectivities of mixed CO_2/CH_4 (50:50) and CO_2/N_2 (10:90) at different temperatures were calculated based on the ideal adsorbed solution theory (IAST) proposed by Myers and Prausnitz.[8] In order to predict the sorption performance of this HOF toward the separation of binary mixed gases, the parameters fitted from the single-component CO_2, CH_4, and N_2 adsorption isotherms based on the dual-site Langmuir-Freundlich (DSLF) model were used in the IAST calculations.[9] The fitting parameters of the DSLF equation are listed in Table S4.

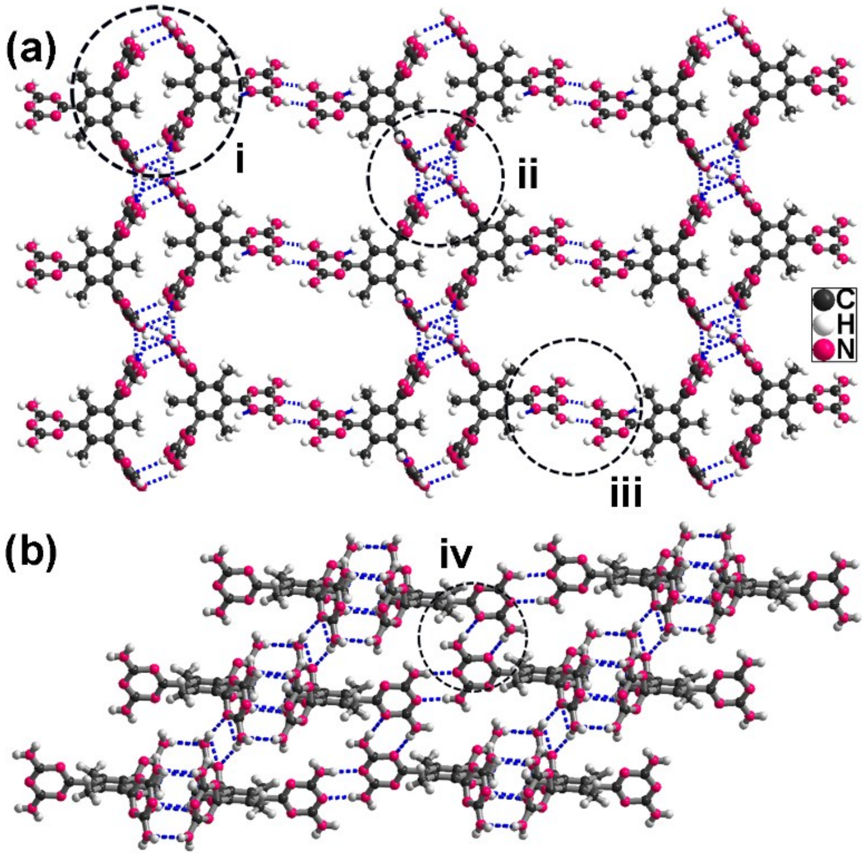

Figure S1. X-ray crystal structure of HOF-9 (a and b) showing the weak connections in a two-dimensional supramolecular layer: hydrogen-bonding interactions (i, ii, and iii) in supramolcecular square and the hydrogen-bonding interactions (iv) between the neighboring supramolecular layers (C: black, N: pink, H: white, water molecules are omitted for clarity).

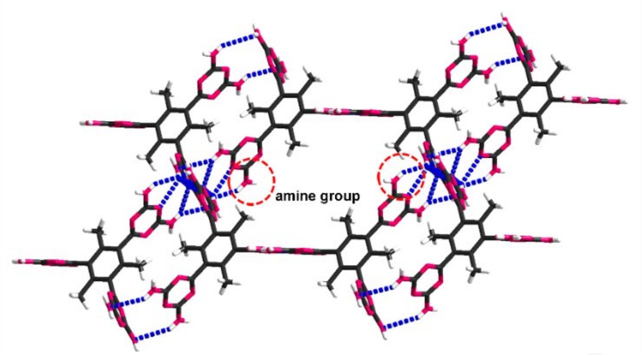

Figure S2. X-ray crystal structure of HOF-9 showing the amine groups decorated on the channels (C: black, N: pink, H: white, water molecules are omitted for clarity).

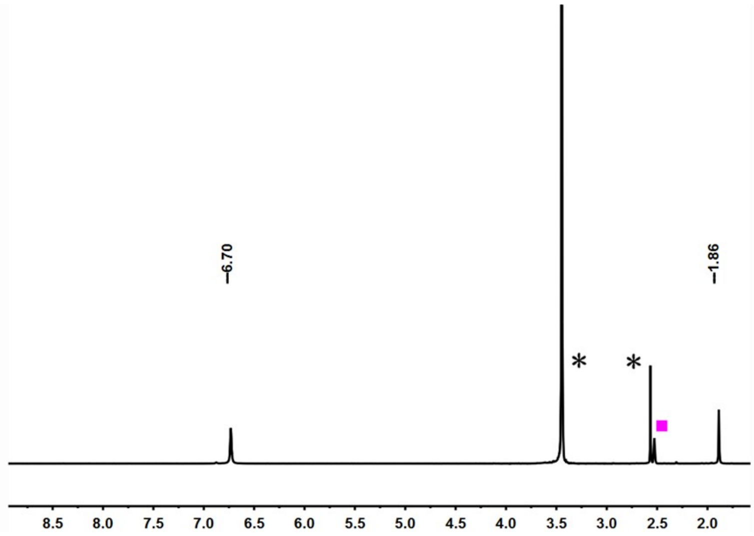

Figure S3. ^{1}H NMR spectrum of HOF-9 (DMSO: square). * denotes DMSO-d_6 solvent impurity.

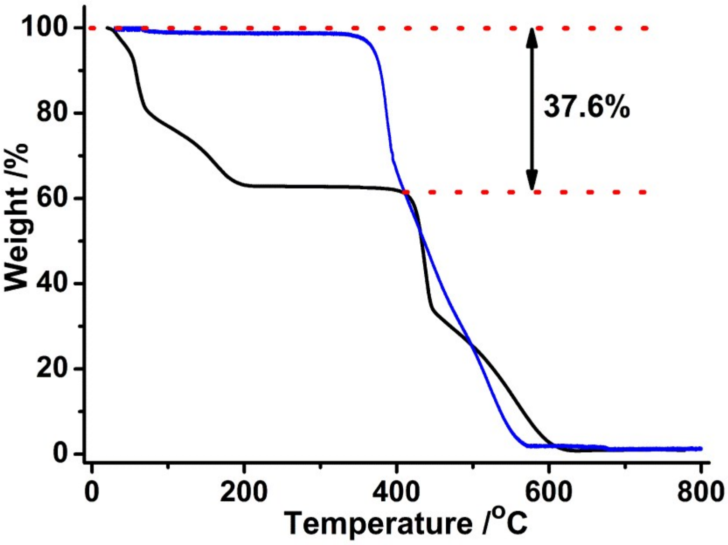

Figure S4. TGA curves of HOF-9 (black line) and HOF-9a (blue line) in the range of 25-800°C.

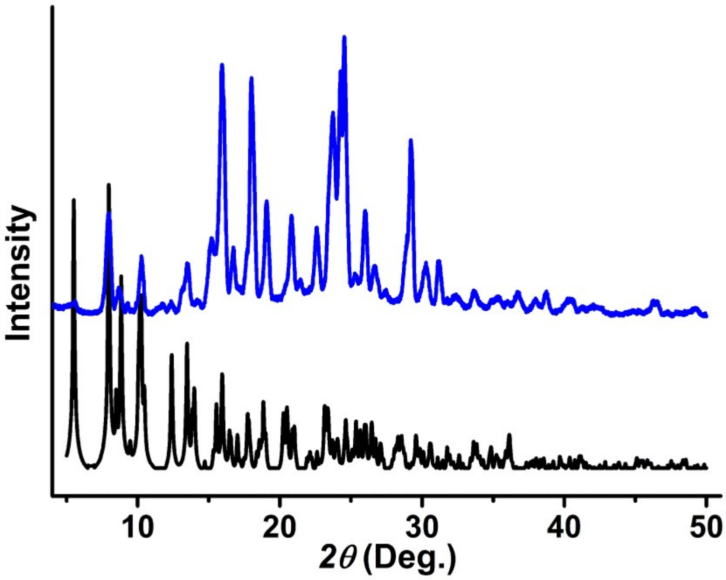

Figure S5. Powder X-ray diffraction profile of as-synthesized HOF-9 (blue line), in comparison with a simulated powder pattern based on the single-crystal HOF-9 structure without considering the solvent molecules (black line).

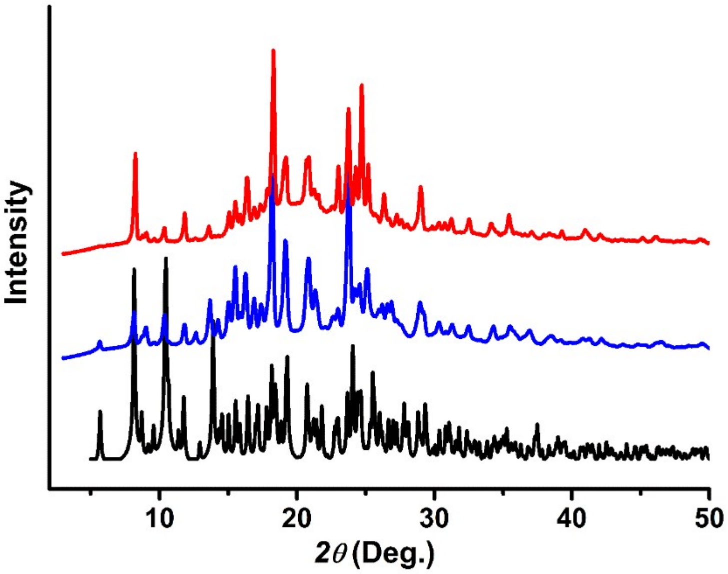

Figure S6. Powder X-ray diffraction profiles for HOF-9⊃Py (blue line) and HOF-9 after soaking in pyridine/toluene (v:v = 1:1, red line) in comparison with a simulated powder pattern based on the single-crystal HOF-9⊃Py structure (black line).

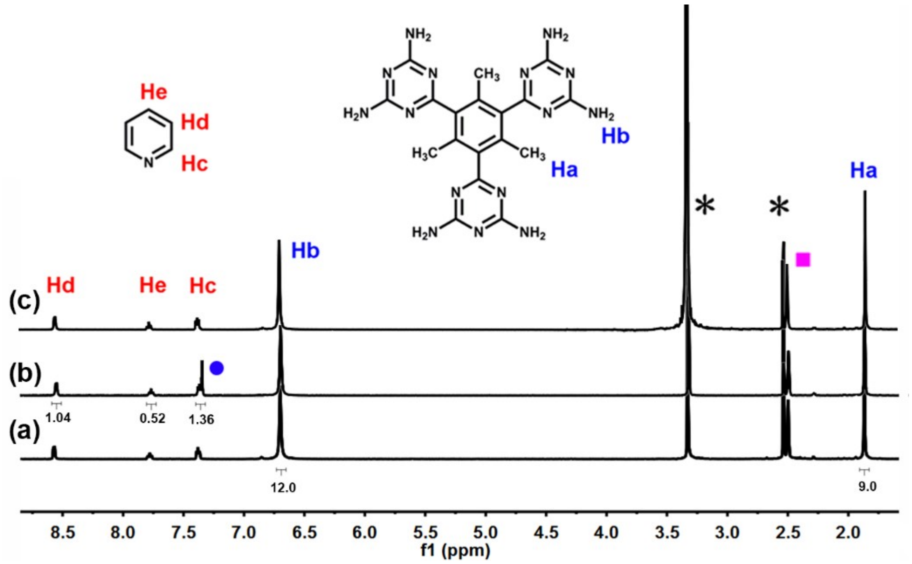

Figure S7. ^{1}H NMR spectra of HOF-9 after soaking in pyridine/toluene (a), pyridine/benzene (b), and pyridine/*p*-xylene (c) in a volume ratio of 1:1. * denotes DMSO-d_6 solvent impurity, pink square denotes DMSO solvent molecules in HOF-9, blue circle denotes proton signal of benzene, which is overlapped with a proton signal of pyridine.

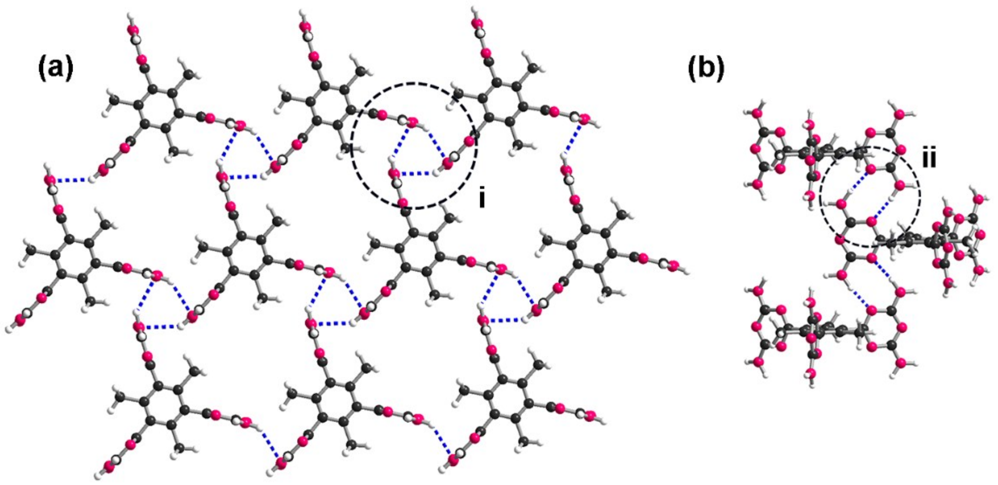

Figure S8. X-ray crystal structure of HOF-9a (a and b) showing the hydrogen-bonding interactions (i and ii) (C: black, N: pink, H: white).

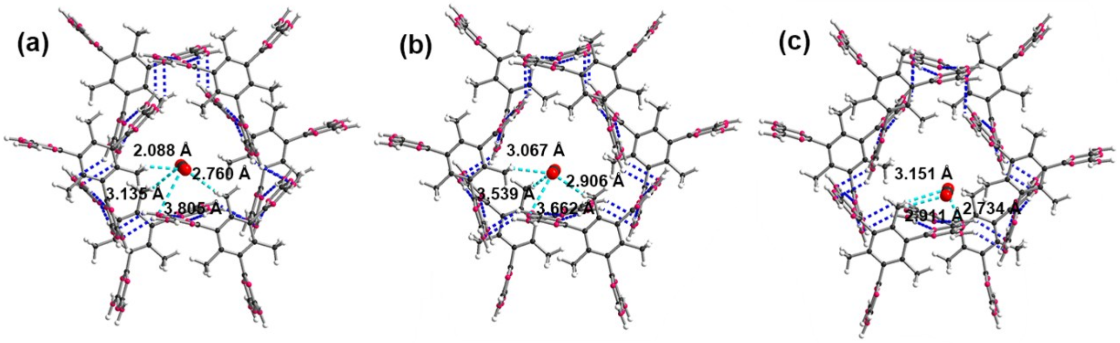

Figure S9. van der Waals interactions (cyan dash line) between CO_2 molecules and HOF-9a in three configurations (a-c) with the binding energies of 32.6, 31.2, and 32.0 kJ/mol, respectively (C: black, N: pink, O: red, H: white).

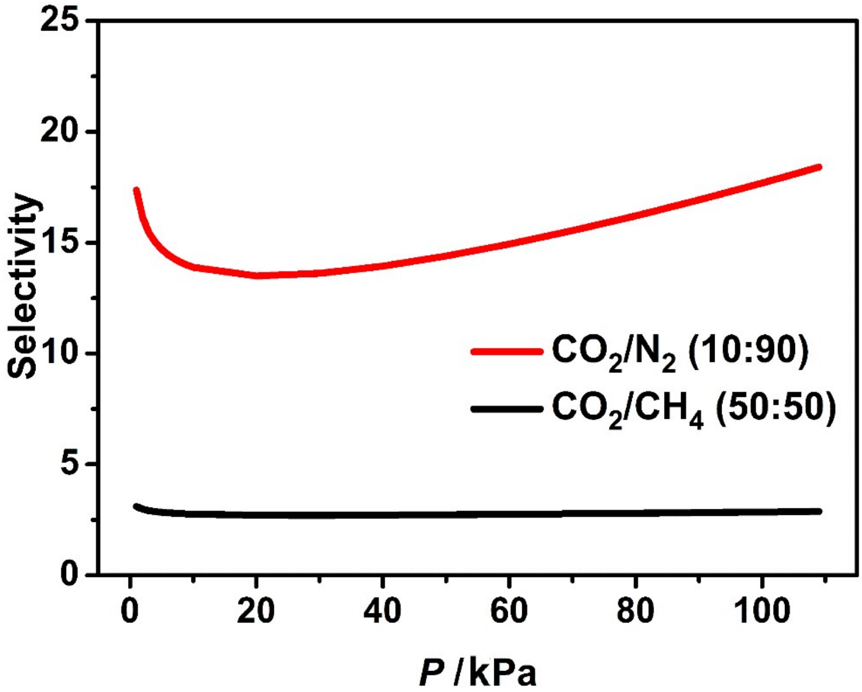

Figure S10. Mixture adsorption selectivity predicted by IAST of HOF-9a for CO_2/CH_4 (50:50) and CO_2/N_2 (10:90) at 296 K.

Table S1. Comparison of the hydrogen bonding interactions and close contact in the crystal structures of HOF-9[a] and HOF-9⊃Py as well as HOF-9a.

D-H···A	distances of D···A (Å) of HOF-9/HOF-9⊃Py	angles of D-H···A (°) HOF-9[a]/HOF-9⊃Py
N1-H1A···N8#1	3.130(3)/3.129(6)	137.3/141.7
N2-H2A···N6#2	3.471(4)/3.588(10)	155.4/143.9
N6-H6B···N10#3	3.042 (3)/3.041(4)	167.7/165.1
N7-H7A···N8#4	3.172(3)/3.119(4)	133.3/139.3
N7-H7A···N3#5	3.288(3)/3.271(6)	139.6/132.8
N11-H11B···N15#6	3.007(3)/3.043(4)	175.2/172.4
N12-H12A···N13#7	2.945(3)/2.957(4)	173.6/173.6
N2-H2B···N16[b]	----/3.200(14)	----/138.2
O1-H1C···N9	2.891(3)/ 2.847(4)	174.7/170.0
O2-H2C···N14	2.798(3)/ 2.796(4)	165.0/163.1
N11-H1A···O1#6	3.068(3)/ 3.057(4)	172.4/173.0
N12-H12B···O1#8	2.856(3)/ 2.829(4)	138.8/137.3
N6-H6A···O2#3	3.071(4)/ 2.991(4)	171.4/176.3
N7-H7A···O2#9	2.874(3)/ 2.879(5)	134.6/ 133.0
D-H···A	distances of D···A (Å) of HOF-9a	angles of D-H···A (°) HOF-9a
N2-H4···N5#1	2.945(3)	173.6(4)
N2-H3···N2#2	3.582(6)	140(4)

[a] The information is summarized on the basis of the collected crystallographic data for HOF-9 in the present case; [b] hydrogen bond between the pyridine and HOF-9 framework in HOF-9⊃Py. Symmetric code for HOF-9 and HOF-9⊃Py, #1: x+1, y-1, z, #2: -x+1, -y+1, -z+1, #3: -x+1, -y+2, -z+1, #4: -x, -y+2, -z+1, #5: x-1, y+1, z, #6: -x+1, -y+2, -z, #7: -x+2, -y+2, -z, #8: x+1, y, z, #9: x-1, y, z. For HOF-9a, #1: y, x, 1-z, #2: 1-y, 1+x-y, z.

Table S2. The crystallographic and refinement parameters for HOF-9, HOF-9⊃Py, and HOF-9a.

crystal data	HOF-9	HOF-9⊃Py	HOF-9a
system	triclinic	triclinic	hexagonal
space group	*P*-1	*P*-1	*P*-62*c*
MF	$C_{24}H_{43}S_3N_{15}O_5$[a]	$C_{28}H_{35}N_{17}O_2$	$C_{18}H_{21}N_{15}$
FW	483.53	641.73	451.49
a /Å	10.7844(13)	10.8777(10)	11.3535(9)
b /Å	11.6088(10)	11.7580(12)	11.3535(9)
c /Å	15.9757(14)	15.7520(13)	11.7010(12)
α /°	79.642(7)	80.409(7)	90
β /°	86.726(9)	86.674(7)	90
γ /°	69.981(9)	68.799(9)	120
volume /Å^3	1848.6(3)	1852.1(3)	1306.22(26)
Z	2	2	2
solvent-accessible void space /%	51[b]	--	22[a]
refinement parameters	$R_1 = 0.0732$[c]	$R_1 = 0.1022$[b]	$R_p = 0.0771$
	$wR_2 = 0.2289$[d]	$wR_2 = 0.3355$[c]	$R_{wp} = 0.1105$

[a] The molecular formula of HOF-9 was calculated based on the TGA; [b] calculation on the basis of the HOF crystal structures using PLATON software[10]; [c] $R_1 = \Sigma|F_o-|F_c||/\Sigma|F_o|$; [d] $wR_2 = [\Sigma w(F_o^2-F_c^2)^2/\Sigma w(F_o^2)^2]^{1/2}$.

Table S3. IAST selectivity of CO_2/CH_4 and CO_2/N_2 for HOF-9a.

mixture	T (K)	mixture proportion	IAST selectivity at 1 atm
CO_2/CH_4	273	50:50	4.6
CO_2/N_2	273	10:90	25.1
CO_2/CH_4	296	50:50	2.9
CO_2/N_2	296	10:90	17.8

Table S4. Equation parameters for the DSLF isotherm model[a].

adsorbates	N_1^{max} (mmol/g)	b_1 (kPa^{-1})	$1/n_1$	N_2^{max} (mmol/g)	b_2 (kPa^{-1})	$1/n_2$
CH_4 (273 K)	1.4527	1.4527	0.88862	0.89568	0.00711	1.18575
CO_2 (273 K)	2.16584	0.02712	0.94457	1.28308	0.0237	1.01068
N_2 (273 K)	0.9647	0.00147	1.17569	0.6529	0.00148	1.16298
CH_4 (296 K)	1.31847	0.00646	0.95161	1.01349	0.00504	1.11994
CO_2 (296 K)	2.03514	0.01268	0.89747	1.47701	0.0093	1.08661
N_2 (296 K)	0.58567	5.52148E-4	1.35727	0.42546	0.0046	1.00374

[a] Dual-site Langmuir-Freundlich (DSLF) model is listed as below:

$$N = N_1^{\max} \times \frac{b_1 p^{1/n1}}{1 + b_1 p^{1/n1}} + N_2^{\max} \times \frac{b_2 p^{1/n2}}{1 + b_2 p^{1/n2}}$$

Where p (unit: kPa) is the pressure of the bulk gas at equilibrium with the adsorbed phase, N (unit: mol/kg) is the adsorbed amount per mass of adsorbent, N_1^{max} and N_2^{max} (unit: mol/kg) are the saturation capacities of sites **1** and **2**, b_1 and b_2 (unit: 1/kPa) are the affinity coefficients of sites **1** and **2**, and n_1 and n_2 represent the deviations from an ideal homogeneous surface.

Reference:

(1) D. Bruns, H. Miura, K. P. C. Vollhardt and A. Stanger, *Org. Lett.* 2003, **5**, 549.

(2) Z. Hou, T. D. P. Stack, C. J. Sunderland and K. N. Raymond, *Inorg. Chim. Acta* 1997, **263**, 341.

(3) F. Helzy, T. Maris and J. D. Wuest, *Cryst. Growth Des*. 2008, **8**, 1547.

(4) G. M. Sheldrick, *Acta Crystallogr. Sect. A* 2008, A**64**, 112.

(5) A. C. Larson and R. B. Von Dreele, *General Structure Analysis System*, Report LAUR 86−748; Los Alamos National Laboratory: Los Alamos, NM, 1994.

(6) P. Giannozzi, S. Baroni, N. Bonini, M. Calandra, R. Car, C. Cavazzoni, D. Ceresoli, G. L. Chiarotti, M. Cococcioni, I. Dabo, A. Dal Corso, S. Fabris, G. Fratesi, S. de Gironcoli, R. Gebauer, U. Gerstmann, C. Gougoussis, A. Kokalj, M. Lazzeri, L. Martin-Samos, N. Marzari, F. Mauri, R. Mazzarello, S. Paolini, A. Pasquarello, L. Paulatto, C. Sbraccia, S. Scandolo, G. Sclauzero, A. P. Seitsonen, A. Smogunov, P. Umari and R. M. Wentzcovitch, *J. Phys.: Condens. Matter* 2009, **21**, 395502.

(7) V. Barone, M. Casarin, D. Forrer, M. Pavone, M. Sambi and A. J. Vittadini, *J. Comput. Chem*. 2009, **30**, 934.

(8) A. L. Myers and J. M. Prausnitz, *AIChE. J.* 1965, **11**, 121.

(9) S. Xiang, Y. He, Z. Zhang, H. Wu, W. Zhou, R. Krishna and B. Chen, *Nat. Commun.* 2012, **3**, 954.

(10) A. L. Spek, *PLATON*, *A Multipurpose Crystallographic Tool*. Utrecht University: Utrecht, the Netherlands, 2005